Disulfide Bond Assignments and Secondary Structure Analysis of Human and Murine Interleukin 10

William T. Windsor,* Rosalinda Syto, Anthony Tsarbopoulos, Rumin Zhang, James Durkin, Samuel Baldwin, Smita Paliwal, Philip W. Mui, Birendra Pramanik, Paul P. Trotta, and Stephen H. Tindall*

Schering-Plough Research Institute, 2015 Galloping Hill Road, Kenilworth, New Jersey 07033

Received February 26, 1993; Revised Manuscript Received May 21, 1993

ABSTRACT: Interleukin 10 (IL-10), which was first discovered by its ability to inhibit the synthesis of various cytokines, most notably γ interferon, from Th1 helper cells, displays pleiotropic immunoregulatory properties. Human and murine IL-10 have a high amino acid sequence identity (*ca.* 73%), which includes the conservation of all four cysteine residues in human IL-10 and the first four out of five cysteine residues for murine IL-10. Chemical analysis was used to determine that both recombinant human and recombinant murine IL-10 contain two disulfide bonds. The disulfide pairs for each were determined by mass spectrometric and reversed-phase HPLC analysis of trypsin-derived polypeptide fragments. The disulfide bond assignments for both species were similar in that the first cysteine residue in the sequence paired with the third and the second paired with the fourth. The fifth cysteine in murine IL-10 was determined by chemical modification to be unpaired. Far-UV circular dichroism analysis indicated that the secondary structure of recombinant human and murine IL-10 are composed of *ca.* 60% α-helix. Reduction of the disulfide bonds structurally destabilized the protein and led to a structure containing only 53% α-helix. The reduced protein displayed no *in vitro* biological activity in a mast cell proliferation assay. These studies indicate that IL-10 is a highly α-helical protein containing two disulfide bonds, either one or both of which are critical for its structure and function. In addition, these properties suggest that this interesting cytokine may belong to the α helical cytokine class of hematopoietic ligands.

Interleukin 10 (IL-10),[1] formerly designated cytokine synthesis inhibitory factor (CSIF), was originally identified in the murine system as a product of the type 2 helper T cells (Th2) that inhibited the synthesis of cytokines from activated type 1 helper T cell clones (Th1), including γ interferon, interleukin 2, interleukin 3, tumor necrosis factor β, and granulocyte–macrophage colony-stimulating factor (Fiorentino et al., 1989; Moore et al., 1990). The inhibition of synthesis of these cytokines by IL-10 is apparently mediated through suppression of monocyte/macrophage accessory cell function (Fiorentino et al., 1991; de Wall Malefyt et al., 1991; Howard et al., 1992; Moore et al., 1993). Additional studies have demonstrated that both human and murine IL-10 are highly pleiotropic in their biological effects, exhibiting immunosuppressive effects on monocyte/macrophages as well as immunostimulatory effects on various cell types, including T cells, B cells, and mast cells [reviewed in Howard et al. (1992) and Moore et al. (1993)]. Of special importance is the ability of IL-10 to down-regulate class II major histocompatibility antigen expression on monocytes (de Wall Malefyt et al., 1991) and to stimulate the differentiation of activated B cells into antibody-secreting cells (Rousset et al., 1992; DeFrance et al., 1992; Banchereau et al., 1991). These immunoregulatory properties of IL-10 suggest broad clinical applications, as reviewed by Howard et al. (1992) and Moore et al. (1993), and include its use in prolonging allograft survival, the treatment of a variety of T-cell-mediated autoimmune diseases, and its use as a potent antiinflammatory agent.

The unique and important immunoregulatory properties of IL-10 have warranted an intensive investigation of not only its biological effects but also its biochemical and biophysical properties in order to understand structure–function relationships. The primary sequences have been deduced from the cDNA sequences for both human and murine IL-10 (Moore et al., 1990; Vieira et al., 1991) and contain 160 and 157 amino acids, respectively, with a sequence identity of 73%. Secondary structure analysis predicts that both proteins have high α-helix content.

Sulfhydryl characterization is an important first step for elucidating the biochemical and structural properties of proteins. Human IL-10 contains four cysteines (Cys12, Cys62, Cys108, and Cys114), and murine IL-10 contains five cysteine residues (Cys9, Cys59, Cys105, Cys111, and Cys146). The first four cysteines in the muIL-10 sequence are conserved in huIL-10. We report here the disulfide pairing of recombinant human IL-10 (rhuIL-10) and recombinant murine IL-10 (rmuIL-10) based on analysis of disulfide-paired tryptic fragments using mass spectrometry and RP-HPLC. Circular dichroism measurements indicate that both proteins are highly α-helical, which together with their general biochemical properties suggests that huIL-10 and muIL-10 belong to the α-helical cytokine class of proteins, e.g., interleukin 2, interleukin 4, granulocyte–macrophage colony-stimulating factor, β interferon, and γ interferon (McKay, 1992; Ealick et al., 1991; Walter et al., 1992a,b; Diederichs et al., 1991; Smith et al., 1992; Powers et al., 1992; Senda et al., 1992).

MATERIALS AND METHODS

Cytokines. Recombinant huIL-10 derived from CHO cells contains 160 amino acids and has a predicted molecular mass

* To whom correspondence should be addressed.

[1] Abbreviations: IL-10, interleukin 10; huIL-10, human interleukin 10; muIL-10, murine interleukin 10; rhuIL-10, recombinant human interleukin 10; rmuIL-10, recombinant murine interleukin 10; CD, circular dichroism; GndHCl, guanidine hydrochloride; DTT, dithiothreitol; EDTA, ethylenediaminetetraacetic acid; Tris, tris(hydroxymethyl)aminomethane; Pmc, 2,2,5,7,8-pentamethylchroman-6-sulfonyl; Fmoc, fluorenylmethyloxycarbonyl; tBoc, *tert*-butyloxycarbonyl; RP-HPLC, reversed-phase high-pressure liquid chromatography.

0006-2960/93/0432-8807$04.00/0

of 18 647 Da. Recombinant muIL-10, refolded from *Escherichia coli*-derived inclusion bodies, contains 157 amino acids and has a predicted molecular mass of 18 453 Da. The cDNA predicted N-terminal sequences for rhuIL-10 and rmuIL-10 are Ser-Pro-Gly and Gln-Tyr-Ser, respectively. Both proteins were purified to greater than 95% using conventional chromatography. RhuIL-10 and rmuIL-10 were observed to have apparent molecular masses of ~18 kDa by reducing and nonreducing SDS–polyacrylamide gel electrophoresis.

Chemical Analysis of Free Sulfhydryl and Disulfide Content. The sulfhydryl content was determined using 4,4′-dithiodipyridine (Aldrich, Milwaukee, WI) under denaturing conditions as described by Grassetti and Murray (1967). Reactions were performed at room temperature for 15 min and used 25–100 μg per 750-μL reaction volume. The moles of free sulfhydryl were calculated from the increase in absorbance at 324 nm, corrected by a solvent blank, using a molar extinction coefficient of 1.98×10^4 M^{-1} cm^{-1}. Control experiments using bovine serum albumin (Calbiochem, San Diego, CA) yielded 0.655 ± 0.058 sulfhydryls per mole of protein and was similar to previously published values (Grassetti & Murray, 1967; Windsor et al., 1991). The disulfide content was determined by using disodium 2-nitro-5-thiosulfobenzoate (Aldrich, Milwaukee, WI) in the presence of excess sodium sulfite and 4–6 M GndHCl (Thannhauser et al., 1984; Damodaran, 1985). Similar amounts of protein were used as described for the free sulfhydryl determination; however, the amount of cystine was determined from the increase in absorbance at 412 nm using an extinction coefficient of 1.36×10^4 M^{-1} cm^{-1}. Control experiments using lysozyme and ribonuclease (Sigma, St. Louis, MO), which contain four disulfide bonds each, yielded values of 4.08 ± 0.053 and 4.14 ± 0.16 cystines per mole of protein, respectively (Thannhauser et al., 1984; Damodaran, 1985; Windsor et al., 1991). Data are expressed per mole of human or murine IL-10, respectively, and are the mean of four to eight replicates ±1 SD.

Disulfide Pairing. Tryptic cleavage of human and murine IL-10 conveniently cleaves between each of the four cysteines in huIL-10 and each of the five cysteines in muIL-10 (Tables I, II, and III). Prior to tryptic cleavage of rmuIL-10, the free cysteine residue was alkylated with iodoacetic acid (Sigma, St. Louis, MO) to minimize potential disulfide scrambling during the tryptic cleavage reaction. This method was effective in preventing scrambling since digests of samples not alkylated resulted in the detection of nearly all potential disulfide pairs, while the alkylated treated samples had only two disulfide pairs, as expected. Alkylation of rhuIL-10 was not performed routinely; however, alkylation controls were performed to eliminate the potential of disulfide scrambling, and the results from these experiments were identical to the non-alkylated studies. Alkylation was carried out using 0.3 mg/mL human or murine IL-10 (500 μg) in 0.2 M Tris, 4 M GndHCl (ultrapure; Schwartz/Mann, Cambridge, MA), and 2 mM EDTA, pH 8.1, with 0.1 M iodoacetic acid for 40 min at room temperature in the dark. The reaction was stopped by adding 1% acetic acid followed by desalting of the buffer components and reagents using a C8 column (Rainin, Dynamax 300 Å, 4.6 mm i.d. × 25 cm) by reversed-phase high-pressure liquid chromatography (RP-HPLC). Desalting required (1) loading the alkylated protein onto the column; (2) washing the column with buffer A (H_2O and 0.1% trifloroacetic acid, TFA) for 2 min, during which the solvent components eluted; and (3) eluting the sample with a 30-min acetonitrile (ACN) and 0.1% TFA (buffer B) gradient. Following lyophilization, the desalted sample was resuspended in the digestion buffer and

Table I: Sequences and Mass Values of Trypsin-Derived HuIL-10 Peptides[a]

fragment	sequence	predicted[b] MH+	obsd[c] MH+	Cys no.
T1	^{1}SPGQGTQSENSCTHFPGNLPN MLR^{24}	2573.8	2573.0	C12
T2	^{25}DLR^{27}	403.5		
T3	^{28}DAFSR^{32}	595.6	595.2	
T4	^{33}VK^{34}	246.3		
T5	^{35}TFFQMK^{40}	802.0	801.5	
T6	^{41}DQLDNLLLK^{49}	1072.2	1071.5	
T7	^{50}ESLLEDFK^{57}	981.1	980.6	
T8	^{58}GYLGCQALSEMIQFYLEEVMP QAENQDPDIK^{88}	3562.0	3565.7	C62
T9	^{89}AHVNSLGENLK^{99}	1182.3	1182.4	
T10	^{100}TLR^{102}	389.5		
T11	^{103}LR^{104}	288.4		
T12	^{105}LR^{106}	288.4		
T13	^{107}R	175.2		
T14	^{108}CHR^{110}	415.5		C108
T15	^{111}FLPCENK^{117}	851.0	849.9	C114
T16	^{118}SK^{119}	234.3		
T17	^{120}AVEQVK^{125}	673.8	673.1	
T18	^{126}NAFNK^{130}	593.7	595.2	
T19	^{131}LQEK^{134}	517.6		
T20	^{135}GIYK^{138}	480.6	480.5	
T21	^{139}AMSEFDIFINYIEAYMTMK^{157}	2318.7	2319.5	
T22	^{158}IR^{159}	288.4		
T23	^{160}N	133.1		

[a] Digestion conditions are described in the Materials and Methods section. [b] Isotopically averaged mass values. [c] Mass values observed from the nonreduced tryptic digest of rhuIL-10 shown in Figure 1. This list does not include the observed disulfide pairs (see Table II).

Table II: Predicted and Observed Trypsin-Derived HuIL-10 Disulfide-Paired Masses under Nonreducing Conditions[a]

	corresponding fragment pair[b]	predicted MH+ [c]	obsd MH+
obsd disulfide pair			
C12–C108	T1–T14	2986.3	2,988.3[d]
	T1–T13, 14	3142.5	3,148.9[d]
C62–C114	T8–T15	4410.0	4,410.4[d]
potential disulfide pair			
C12–C62	T1–T8	6132.8	none
C12–C114	T1–T15	3421.8	none
C62–C108	T8–T14	3944.5	[e]
	T8–T13, 14	4130.7	none
C108–C114	T14–T15	1263.5	none
	T13, 14–T15	1419.7	none

[a] HuIL-10 was digested with trypsin, and the nonreduced fragment masses were detected by using plasma desorption mass spectrometry. [b] Fragment nomenclature is defined in Table I. Fragment pairs containing R107 (T13) indicate that incomplete trypsin cleavage occurred between R107 and the disulfide-paired C108. [c] Isotopically averaged mass values. [d] Nonreduced; full reduction of these samples with 0.1 M DTT at 37 °C for 1 h led to the complete loss of masses corresponding to the cystine fragment pairs and led to an increase in the individual cysteine fragment masses, thereby confirming the identity of the disulfide-paired fragments. In addition, no masses corresponding to potential homocysteine dimers were detected. [e] On occasion a small peak was observed containing a mass value consistent with this cystine pair. HPLC analysis indicated the amount was less than 4% of the C62–C114 pair.

treated with trypsin, as described below. For samples not alkylated, the protein was prepared by dialyzing overnight into 0.1 M ammonium bicarbonate, pH 8.1.

Human and murine IL-10 were digested (100–500 μg) in 0.1 M ammonium bicarbonate, 2 M urea (Boehringer Mannheim, Indianapolis, IN), and 2 mM $CaCl_2$, pH 8.1, at a concentration of 0.3 mg/mL. Digestion with trypsin (sequencing grade; Boehringer Mannheim, Indianapolis, IN) was initiated by adding trypsin at a 1:20 (w/w) trypsin:IL-10 ratio at 37 °C followed by another 1:20 addition 4 h later and a 1:40 addition after 20 h. After 23–28 h the reaction was stopped by adding acetic acid to 1%. Tryptic peptide fragments

Table III: Predicted and Observed Trypsin-Derived MuIL-10 Disulfide-Paired Masses under Nonreducing Conditions[a,b]

obsd disulfide pair	corresponding fragment pairs: sequence	corresponding fragment pairs: predicted reduced mass (MH^+)	predicted cystine–paired mass (MH^+)	obsd mass (MH^+) (nonreduced)[c,d]
C9–C105	^{5}EDNNCTHFPVGQSHMLLELR^{24}	2341.6	2754.1	2754.2
	^{105}CHR^{107}	415.5		
C9–C105	^{5}EDNNCTHFPVGQSHMLLELR^{24}	2340.6	2910.3	2910.2
	^{104}R + ^{105}CHR^{107}	571.4		
C59–C111	^{55}GYLGCQALSEMIQFYLVEV MPQAEK^{79}	2849.4	3697.4	3697.3
	^{108}FLPCENK^{114}	851.0		

[a] See Table II for an explanation of this table. [b] MuIL-10 was alkylated prior to trypsin digestion, and a strong MH^+ peak was observed at 2354.2, corresponding to an alkylated fragment containing a carboxymethylated fifth cysteine, Cys146. [c] No other disulfide-paired masses were detected. [d] Following reduction with 0.1 M DTT and 0.1 M ammonium bicarbonate, pH 8.1, at 37 °C for 1 h, these masses disappeared and the mass peaks corresponding to peptides containing C9 and C59 increased in intensity, which strongly suggested that these masses contained cystine-paired peptides.

were desalted from buffer components by RP-HPLC, as described above, except that the sample was eluted from a C18 column (Rainin, Dynamax 300 Å, 4.6 mm i.d. × 25 cm) with an isocratic elution containing 80% ACN/TFA, which was sufficient to elute all of the trypsin-derived peptides. Peptides were lyophilized and prepared for mass spectrometric analysis as described below.

Mass Spectrometry. Plasma desorption mass spectra were obtained using a BIOION 20 californium-252 plasma desorption time-of-flight mass spectrometer and an accelerating voltage of 18 kV (Sundqvist et al., 1984; Tsarbopoulos et al., 1988). Total IL-10 tryptic digests were prepared for plasma desorption mass spectrometry (PDMS) by resuspending the lyophilized digested sample (1–10 nmol) obtained from the RP-HPLC isocratic elution in a 1:2 (v/v) mixture of ethanol: 0.1% aqueous TFA; the mixture was applied to a nitrocellulose-coated (NC-coated) aluminum foil and spin-dried prior to analysis. Further thorough rinsing of the NC-absorbed peptide mixture with 0.1% TFA or deionized water enhanced the signals of the higher mass peptide fragments (Tsarbopoulos, 1989). Reduced fragments were generated by resuspending lyophilized total digests in 0.1 M ammonium bicarbonate, pH 8.1, and 0.1 M DTT (Aldrich, Milwaukee, WI), incubating the sample for 1 h at 37 °C, and making a 1:1 (v/v) mixture of the reduced sample with the ethanol/TFA solution described above. The time-of-flight spectra were acquired over a 1–3-h period and converted to mass spectra using the centroids for H^+ and NO^+ as calibration peaks. Complete tryptic digestion of the protein appeared to have occurred since incomplete digestion fragments were rarely observed, and SDS–PAGE as well as reversed-phase HPLC chromatograms were consistent with complete digestion.

RP-HPLC Chromatography. RP-HPLC chromatography was performed using a Rainin Dynamax System (Rainin, Woburn, MA) consisting of two HPX-5SC pumps, a mixer, and a Knauer variable-wavelength detector interfaced to a Macintosh SE computer. Well-resolved RP-HPLC chromatograms of trypsin-derived IL-10 polypeptide fragments or synthetic peptides were obtained using a C18 column (Rainin Dynamax 300 Å, 0.46 mm i.d. × 25 cm) developed with a water–acetonitrile gradient containing 0.1% trifluoroacetic acid (ACN/TFA) and run at a flow rate of 1 mL/min. Samples loaded onto the column were either preequilibrated with equal volumes of buffer A (0% ACN, 0.1% TFA) or adjusted to 1% acetic acid. Loaded samples were initially washed for 2 min with buffer A followed by a 2-h 20–55% ACN/TFA gradient. The chromatograms were well resolved using approximately 75 μg of rhuIL-10 digests or 5–10 μg of each synthetic peptide. The reduced chromatograms were obtained by reacting either the IL-10 digests or oxidized synthetic peptides with 0.1 M DTT for 1 h at room temperature or 37 °C. All chromatograms were obtained at room temperature, and peptide elution was detected by UV absorbance at 215 nm using a Knauer (Model 87) variable-wavelength detector.

Partial Reduction Studies of Intact huIL-10. The RP-HPLC chromatograms of nonreduced and reduced intact (nondigested) rhuIL-10 were obtained using a C8 column (Rainin Dynamax 300 Å, 4.6 mm i.d. × 25 cm) eluted with a 20–40% ACN/TFA gradient over 30 min. Severe protein precipitation occurred upon reduction at concentrations near 1 mg/mL. Therefore, all of the reduction studies were performed at less than 0.1 mg/mL, where no precipitation was visible. Reduced and nonreduced protein samples were adjusted to 1% acetic acid prior to chromatography to stop the reduction reaction and to denature the sample prior to chromatography.

Partially reduced rhuIL-10 intermediates could be generated under non-denaturing conditions by incubating the sample with 0.3 mM DTT for 5–10 min at room temperature. Partially reduced samples were purged with nitrogen gas to minimize reoxidation by oxygen. Intermediates I1 and I2 could be resolved on a C8 column and had elution times between those of the native and the fully reduced species under the chromatography conditions described above. To determine which disulfide was reduced in I1 or I2, we purified and lyophilized each species under acidic conditions. The lyophilized samples were resuspended in 0.25 M Tris, 4 M GndHCl, and 2 mM EDTA, pH 8.5, containing 0.01 or 0.1 M iodoacetic acid and alkylated in the dark for 15 min at room temperature. The reagents were then removed by desalting on a gel-filtration column which was equilibrated with 0.1 M ammonium bicarbonate and 2 M urea, pH 8.1. Tryptic digestion and RP-HPLC on a C18 column was then performed as described in the Disulfide Pairing section to determine which disulfides were reduced on the basis of the absence or presence of cystine- or cysteine-containing peaks (see Figure 2).

Peptide Synthesis. Four peptides corresponding to the huIL-10 tryptic fragments containing each of the four cysteine residues (T1, T8, T14, and T15 in Table I) were synthesized on an automated ABI 431A peptide synthesizer (Applied Biosystems, Foster City, CA) using the vendor's FastMoc FMOC chemistry protocol. Arginine and lysine side-chain groups were protected with Pmc and *t*-Boc, respectively (Applied Biosystems, Foster City, CA). Cysteine, asparagine, glutamine, and histidine side chains were protected by trityl groups, and all other trifunctional amino acid residue side chains were protected with *tert*-butyl groups (Applied Biosystems, Foster City, CA). Peptides were cleaved and deprotected at room temperature for 1.5 h in a solution containing 82.5% TFA, 5% H_2O, 5% thioanisole, 5% phenol,

and 2.5% ethanedithiol (chemicals from Aldrich, Milwaukee, WI). Cleaved peptides were precipitated with ice-cold anhydrous ethyl ether, resuspended in 5% acetic acid, and lyophilized. Purification was performed by RP-HPLC with a C8 column (Rainin Dynamax 300 Å, 41.4 mm i.d. × 25 cm) using an acetonitrile gradient in 0.1% TFA. The molecular masses of the purified peptides were confirmed by mass spectrometry.

The four cysteine-containing synthetic peptides, T1, T8, T14 and T15, were oxidized in pairs and alone to generate all possible hetero- and homodimeric disulfide pairs. Oxidation reactions were catalyzed with oxygen in an open-air container with stirring in 10 mM Tris, 0.2 M NaCl, and 0.02% sodium azide, pH 8. The extent of air oxidation was monitored by RP-HPLC, and for reactions involving T14 the reaction was more than 95% complete with only an overnight reaction. Air oxidations involving peptides other than T14 took 5 days to obtain greater than 70% completion.

Circular Dichroism. CD spectra were recorded on an IBM-interfaced Jasco 500A spectropolarimeter. Spectra were recorded at room temperature by using either a 0.1-cm-path-length cell for far-UV CD measurements of samples containing protein concentrations between 0.03 and 0.1 mg/mL or a 1.0-cm cell for the near-UV CD measurements, in which 0.5–1 mg/mL samples were used. Each spectrum was averaged from eight scans at a rate of 20 nm/min and a time constant of 1 s. A solvent spectrum was subtracted from each protein spectrum. Reported spectra are expressed as mean residue ellipticity, $[\theta]_{MRW}$, and are calculated by using a mean residue weight of 116.5 for both human and murine IL-10. The spectropolarimeter was calibrated using ammonium *d*-10-camphorsulfonate (Aldrich, Milwaukee, WI) as described by Takakuwa et al. (1985). All samples were clarified prior to analysis either by centrifugation or through filtration using a 0.22-μm GV Millipore filter. Analysis of the mean residue ellipticity spectra for the percent secondary structure was performed using the method of Chang et al. (1978).

Concentration Determination. Protein concentrations for rhuIL-10 and rmuIL-10 were determined by amino acid compositional analysis. Protein samples were hydrolyzed in 6 N HCl at 150 °C for 1 h using a Waters Picotag station. Samples were analyzed using a Hewlett-Packard AminoQuant II system. All reagents and standards were purchased from Hewelett-Packard (Waldbronn, Germany). An absorbance molar extinction coefficient at 280 nm was also determined by measuring a baseline-corrected absorbance spectrum for rhuIL-10 in 10 mM sodium phosphate, pH 7.0, followed by elucidation of the protein concentration using amino acid analysis as described above. The extinction coefficient at 280 nm obtained by this method was 8740 M^{-1} cm^{-1} (or $\epsilon^{0.1\%}$ = 0.47 mg^{-1} cm^2), and this value was used for determining the protein concentration in all of the CD studies.

Bioactivity. The biological activity of both murine and human IL-10 was determined using the murine mast cell proliferation (MC/9) assay costimulated with murine interleukin 4 (O'Garra et al., 1990). Native and reduced samples were diluted 1000-fold directly into the assay media and frozen until assayed.

RESULTS AND DISCUSSION

Sulfhydryl Analysis. Initial biochemical characterization of rhuIL-10 and rmuIL-10 involved sulfhydryl analysis, which included the determination of both the free sulfhydryl content and the number of disulfide bonds for each protein. Human IL-10 contains four cysteines (Cys12, Cys62, Cys108, and Cys114), and murine IL-10 contains five cysteine residues (Cys9, Cys59, Cys105, Cys111, and Cys146). The number of free cysteine residues in rhuIL-10 was determined by chemical analysis using 4,4′-dithiodipyridine and 4 M GndHCl under denaturing conditions. The results from this sulfhydryl-specific reaction indicated that rhuIL-10 contained 0.014 ± 0.007 mol of sulfhydryl/mol of rhuIL-10. A similar reaction was performed for rmuIL-10, and the results indicated that this species contained 1.03 ± 0.1 mol of sulfhydryl/mol of rmuIL-10.

Direct measurement of the disulfide bond content was obtained by reaction with 2-nitro-5-thiosulfobenzoate (Thannhauser et al., 1984; Damadoran, 1985) under denaturing conditions using 4 M GndHCl. Analysis of this reaction indicated that rhuIL-10 contained 2.15 ± 0.068 mol of cystine/mol of rhuIL-10. The value determined for rmuIL-10 was 2.59 ± 0.25 mol of cystine/mol of rmuIL-10. These results, along with the results for the free sulfhydryl content as well as the high sequence homology, provided strong evidence that rhuIL-10 and rmuIL-10 each contained 2 disulfide bonds and that a fifth cysteine in rmuIL-10 existed as a free sulfhydryl.

Disulfide Bond Assignment. (A) Mass Spectral Analysis. The specific disulfide pairing for both rhuIL-10 and rmuIL-10 was determined by proteolytic digestion of the protein followed by identification of disulfide pairs by either mass spectrometry or RP-HPLC chromatography. Digestion of both rhuIL-10 and rmuIL-10 with trypsin is predicted to generate 23 fragments and to cleave between each of the cysteine residues (Tables I and III). Four of the cysteine-containing fragments are predicted to generate two discrete disulfide-bonded polypeptides. It was found that in order to obtain complete digestion of IL-10, the reaction had to be performed under partially denaturing conditions using 2 M urea (see Materials and Methods). Mass analysis of the digests using plasma desorption mass spectrometry was performed to identify the unique disulfide paired polypeptides. Panels A and B of Figure 1 show the ionization spectra for the low- and the high-mass range, respectively, of the nonreduced rhuIL-10 total tryptic digest purified by RP-HPLC. The low-mass range (Figure 1A) contained all of the expected peptide fragments with masses between 450 and 1800 Da (Table I) except T19 (m/z 517.6), which due to its highly polar content may not have bound to the C18 column during the purification step. The higher mass range (Figure 1B) contained two signals with m/z values of 2988.3 and 4410.4, which coincided with the predicted disulfide pairs of Cys12–Cys108 (2986.3 MH^+) and Cys62–Cys114 (4410 MH^+), respectively (Tables I and II). These disulfide bond assignments were confirmed in Figure 1C, where, following reduction of the digested sample with 0.1 M DTT at 37 °C for 1 h, the mass spectrum was devoid of these cystine-containing signals and enriched in the free-cysteine-containing signals at m/z 851, 2574, and 3562. Tables I and II contain a summary of the observed masses shown in Figure 1. In general, all of the predicted tryptic masses above 450 Da were observed, and only under less stringent conditions (i.e., short digestion times or digestion in the absence of urea) were incomplete digestion fragments detected. Exceptions were the signal at m/z 3148.9, which corresponded to the Cys12–Cys108 (T1–T14) dislufide pair containing the incompletely cleaved Arg107 (T13) residue that is adjacent to the disulfide bond, and a minor peak at m/z 659.5 containing T10,11. Similar results were also observed for samples that were alkylated with iodoacetic acid prior to tryptic digestion, providing supporting evidence that no free sulfhydryl–disulfide interchange occurred during the

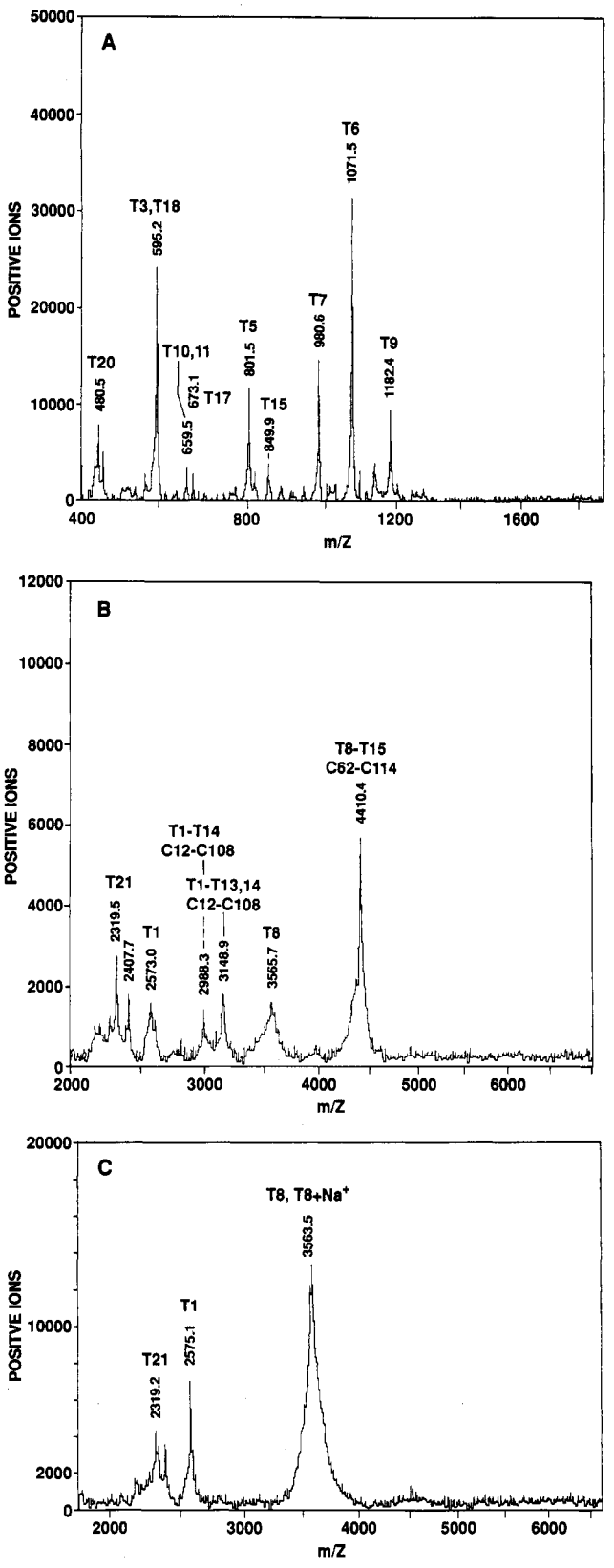

FIGURE 1: Plasma desorption mass spectrum of rhuIL-10 tryptic digests under nonreducing and reducing conditions. (A) Trypsin-derived rhuIL-10 fragments observed in the low-mass range (400–2200 MH^+) under nonreducing conditions. (B) Trypsin-derived rhuIL-10 fragments observed in the high-mass range (2000–7000 MH^+) under nonreducing conditions. (C) Observed masses corresponding to the 0.1 M DTT reduced rhuIL-10 tryptic digest sample from (B) in the high-mass range (1800–7000 MH^+).

23-h digestion. The only significant mass unassigned was at m/z 2407.7 (Figure 1B) and may be an incomplete cleavage product since its relative amount was variable from different cleavage preparations.

The disulfide pairing analysis using PDMS consistently showed intense signals for the Cys62–Cys114 pair, while the signal corresponding to the Cys12–Cys108 pair was significantly lower. This difference may be related to selective desorption of the former disulfide pair over the latter. This may arise from possible differences in amino acid composition, such as the Cys62–Cys114 pair containing nine acidic residues (five glutamic and two aspartic acid residues) while the Cys12–Cys108 pair contains only one acidic residue (glutamic acid).

Disulfide analysis was also performed for rmuIL-10. Prior to digestion the free cysteine residue was alkylated with iodoacetic acid under denaturing conditions (4 M GndHCl). Table III contains a summary of the observed masses for the PDMS analysis of the nonreduced digest. It was observed that following tryptic digestion rmuIL-10 contained two fragments with masses of 2754.2 and 3697.3 Da, consistent with the predicted Cys9–Cys105 (2754.1 Da) and Cys59–Cys111 (3697.4 Da) pairings, respectively (Table III; data not shown). Upon reduction with 0.1 M DTT these masses were absent from the spectrum, as expected for disulfide-paired fragments. No other potential disulfide pairs were detected. These results indicated that both the rhuIL-10 and rmuIL-10 proteins contained similar disulfide pairings, as was predicted due to their high sequence homology and conservation of cysteines. Thus, disulfide pairings occur between the first cysteine residue in the sequence and the third cysteine residue and between the second cysteine residue in the sequence and the fourth cysteine residue.

(*B*) *RP-HPLC Analysis.* The unique disulfide pairing for rhuIL-10 was further confirmed through a comparison of the RP-HPLC chromatography elution profile of nonreduced trypsin digested rhuIL-10 to that of the elution profile of 10 different synthetic peptide disulfide pairs. The C18 RP-HPLC chromatograms of rhuIL-10 tryptic digests under nonreduced and reduced conditions are shown in panels A and B, respectively, of Figure 2. Peaks N1 and N2 were the only two peaks that shifted upon reduction of the nonreduced sample, implying that these elution peaks contained the two disulfide pairs. In the reduced chromatogram, Figure 2B, three new peaks were resolved, R1, R2, and R3, and were likely to arise from the cysteine fragments T1, T8, and T15. The highly hydrophilic tripeptide T14 probably eluted early within the solvent peaks since the corresponding synthetic peptide (T14) eluted at the solvent front.

Four synthetic peptides were made with sequences corresponding to the four trypsin-derived cysteine-containing polypeptides, T1, T8, T14, and T15 (Table I). These cysteine-containing synthetic peptides were oxidized in pairs or alone to generate all 10 possible disulfide pairs, and the elution time of each pair was compared to that of peaks N1 and N2 of nonreduced rhuIL-10. Oxidation of peptides T1 and T14 generated the Cys12–Cys108 disulfide pair, while a separate oxidation of T8 and T15 produced the Cys62–Cys114 disulfide pair. Figure 2C shows the composite chromatogram of both oxidized reactions containing the Cys12–Cys108 and Cys62–Cys114 co-oxidized peptide pairs. The peaks in this chromatogram were specifically identified with respect to each unique peptide and disulfide pair through an analysis of the elution pattern of all of the reduced and co-oxidized pairs (data not shown). A comparison of nonreduced rhuIL-10 (Figure 2A) and oxidized peptide chromatograms (Figure 2C) revealed that peak N1 corresponded to the Cys62–Cys114

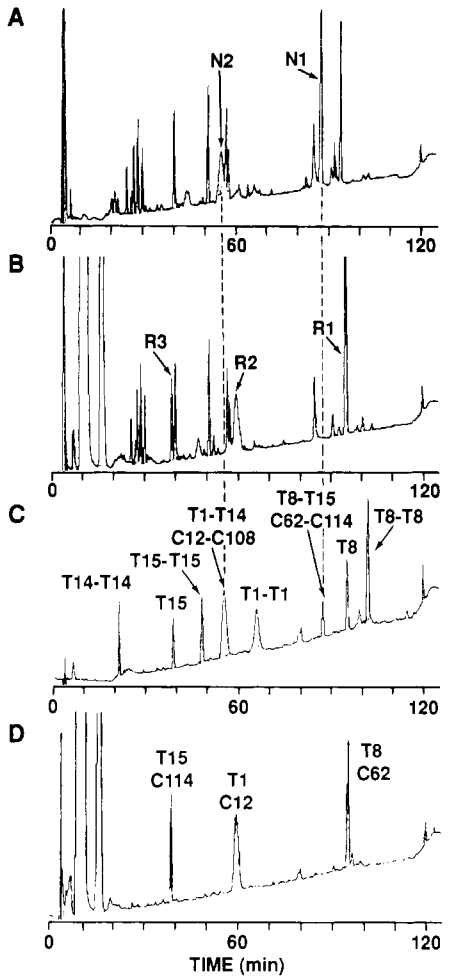

FIGURE 2: RP-HPLC chromatograms of rhuIL-10 tryptic digests and synthetic peptide disulfide pairs run under nonreducing and reducing conditions. (A) Tryptic digest of rhuIL-10 under nonreducing conditions (50 μg of rhuIL-10). (B) Tryptic digest of rhuIL-10 under reducing conditions (0.1 M DTT, 37 °C, 1 h, 50 μg of rhuIL-10 in 50 mM ammonium bicarbonate, pH 8.1). (C) Chromatogram containing the oxidized synthetic peptide disulfide pairs T1–T14 (Cys12–Cys108) and T8–T15 (Cys62–Cys114) under nonreducing conditions. Peptides T1 and T14 and peptides T8 and T15, respectively, were co-oxidized and then mixed together under acidic conditions just prior to chromatography. Peak assignments were determined from chromatograms of each peptide (data not shown). (D) Chromatogram of the synthetic disulfide-paired samples in (C) following reduction with 0.1 M DTT (37 °C, 1 h, 50 mM ammonium bicarbonate, pH 8.1). Approximately 5–10 μg of each peptide was used.

disulfide pair and peak N2 contained the Cys12–Cys108 pair. Similar comparisons between the chromatograms of reduced rhuIL-10 (Figure 2B) and the reduced disulfide-paired synthetic peptides (Figure 2D) revealed that the reduced rhuIL-10 peak R1 contained the T8 (Cys62) peptide, R2 contained the T1 (Cys12) peptide, and R3 was the T15 (Cys114) peptide. The reduced T14 (Cys108) peptide eluted early in the solvent peaks. This RP-HPLC-derived disulfide bond assignment confirmed the results obtained by PDMS.

It is interesting to note that the N2 or the T1–T14 (Cys12–Cys108) peak width was unusually broad compared to peaks corresponding to the other fragments. Peptide T1 (Cys12) has the same characteristic broad shape (Figure 2D); thus the shape of N2 and T1–T14 (Cys12–Cys108) is due to T1. It may be speculated that cis–trans isomerizations of the three proline residues in peptide T1 being slow on the RP-HPLC time scale (2 h) may have caused the peptide to have heterogeneous conformations that interact slightly differently with the column matrix. Such differential column interactions can lead to peak broadening.

One of the main objectives for having performed this elaborate HPLC analysis of oxidized synthetic peptides was to provide a quantitative method for ascertaining the amount, if any, of unexpected mixed disulfides involving incorrectly paired cysteines. Quantitation of peptide amounts is possible with this HPLC method but not by PDMS analysis. On the basis of the HPLC study it was estimated, by comparing the elution times of all the generated mixed disulfides and analyzing peak areas, that the other potential disulfide pairs were either absent or present in trace amounts, the latter being detected in areas that were less than 4% of the two main disulfide pair areas. The sizes of these peaks were similar to those observed for the background peaks.

Far- and Near-UV Circular Dichroism. Primary sequence secondary structure analysis of huIL-10 suggested the protein contained 75% α-helix, 9% β-sheet, 10% β-turn, and 6% random coil (Chou & Fasman, 1978; Garnier et al., 1978). Secondary structure content of proteins can be estimated from an analysis of the protein's far-UV CD spectrum. The shape and magnitude of the far-UV CD spectrum of rhuIL-10 is consistent with a protein containing a high amount of α-helix (Figure 3A). Secondary structure analysis of the spectrum indicated it contained 61% α-helix, 7% β-sheet, 4% β-turn, and 28% random coil (Chang et al., 1978). The far-UV CD spectrum for rmuIL-10 was very similar to rhuIL-10 (Figure 3A). The secondary structure analysis of the mean residue ellipticity spectrum revealed a composition for rmuIL-10 of 60% α-helix, 4% β-sheet, 8% β-turn, and 28% random coil.

Spectral measurements in the near-UV CD region are sensitive to conformational changes and the stereospecific environment of tyrosine and phenylalanine residues. The near-UV CD spectra for rhuIL-10 and rmuIL-10 (Figure 3B) indicated the optical rotations of these two proteins are significantly different. This result suggests that although four of the five tyrosine residues are conserved in position and the proteins have similar α-helical content, there is a significant difference in the aromatic residues' tertiary conformation and/or environment.

The far-UV CD spectrum of a fully reduced sample was also measured to determine the structural role that the disulfide bonds had in stabilizing the protein. This reduced sample was generated by reacting a nitrogen gas purged sample with 1 mM DTT for 1 h at room temperature. Complete reduction was confirmed by C8 RP-HPLC as described in Figure 4. The spectrum of the fully reduced sample (Figure 3A) had a lower ellipticity between 200 and 230 nm and is an indication that a decrease in α-helix content occurred in the absence of disulfide bonds. Analysis of this spectrum revealed that the secondary structure of the reduced sample now had only 53% α-helix, 2% β-sheet, 11% β-turn, and an increase in random coil structure, to 34%.

Disulfide Reduction Studies. Complete and partial reduction of intact (nondigested) rhuIL-10 under non-denaturing and denaturing conditions were performed to determine the structural and functional roles of the disulfide bonds. Reduction of the disulfide bonds in the presence of 0.1 M DTT (50 mM ammonium bicarbonate, pH 8.1) for 1 h at room temperature or 37 °C under non-denaturing conditions for human and murine IL-10 led to complete loss in biological activity, as determined by the mast cell proliferation assay. These results strongly suggested that intact disulfide bonds were critical for the expression of biological activity.

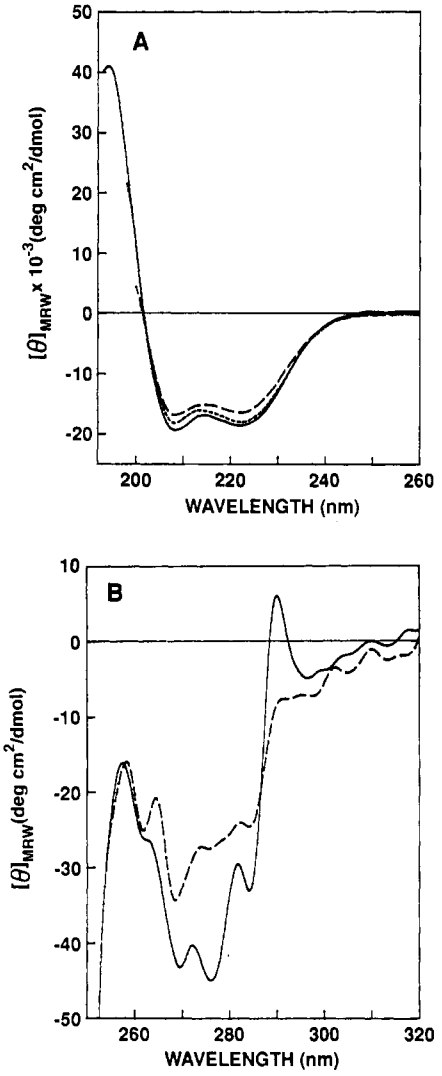

FIGURE 3: Far- and near-UV CD mean residue ellipticity spectra of rhuIL-10 and rmuIL-10. (A) Far-UV CD: (—) rhuIL-10 in 20 mM Tris and 10 mM NaCl, pH 8.1; (- - -) rmuIL-10 in 20 mM Tris and 34 mM NaCl, pH 7.6; (– –) rhuIL-10 reduced with 1 mM DTT for 1 h at room temperature and purged with nitrogen (20 mM Tris and 10 mM NaCl, pH 7.6). The far-UV CD spectrum of the rhuIL-10 sample at pH 7.6 was identical to that of the pH 8.1 sample. (B) Near-UV CD: (—) rhuIL-10 in 20 mM Tris and 10 mM NaCl, pH 8.1; (– –) rmuIL-10 in 20 mM Tris and 0.15 M NaCl, pH 7.6.

Nonreduced and fully reduced rhuIL-10 (0.1 M DTT, 1 h) could be resolved on a C8 RP-HPLC column, as seen in panels A and D of Figure 4, peaks NR and R, respectively. The protein could also be fully reduced under non-denaturing conditions with significantly less reducing agent and shorter time (1 mM DTT for 10 min) at room temperature, and this reduced sample also eluted at peak R. These results are important since they suggested that the disulfide bonds in rhuIL-10 are readily reduced, indicating that at least one disulfide is likely to be exposed to the solvent.

Partially reduced species, purged with nitrogen gas, could be generated under non-denaturing conditions by incubating the sample with only 0.3 mM DTT for 5–10 min at room temperature. Reduction for only 5 min led to a chromatogram containing peak NR with 36% of the area, peak R containing 9% of the area, and two new peaks, I1 and I2, which contained 51% and 4% of the peak area, respectively (Figure 4B). Samples reduced with 0.3 mM DTT for 10 min (Figure 4C) contained less than 6% nonreduced rhuIL-10, peak NR, and 54% fully reduced species, peak R. In addition, the major

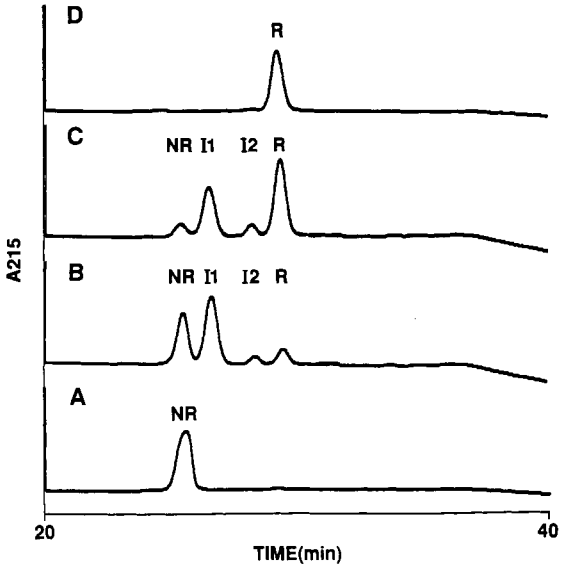

FIGURE 4: RP-HPLC chromatogram of nonreduced, partially reduced, and fully reduced species of rhuIL-10. (A) Elution profile of nonreduced rhuIL-10. (B) Chromatogram of partially reduced rhuIL-10, using 0.3 mM DTT for 5 min. (C) Elution profile of rhuIL-10 reduced with 0.3 mM DTT for 10 min. (D) Chromatogram of fully reduced rhuIL-10, using 1 mM DTT for 10 min. Identical results were obtained for samples reduced with 0.1 M DTT for 1 h. Peaks NR and R correspond to the elution positions of the nonreduced and reduced species, respectively. Peaks I1 and I2 correspond to partially reduced species. Reduction reactions were performed at room temperature in 50 mM ammonium bicarbonate, pH 8.1, using 50 μg of rhuIL-10.

intermediate continued to be peak I1, representing 35% of the total area, while peak I2 continued to be low, <6%. The intermediate elution times of I1 and I2 were consistent with the possibility that each species represented a rhuIL-10 molecule that contained one intact and one reduced disulfide bond. In addition, the large amount of I1 relative to I2 suggested that the reduced disulfide in I1 is more solvent exposed and susceptible to reduction than the other cystine.

To identify which disulfide bond was reduced in I1, the purified sample was digested with trypsin following its alkylation using iodoacetic acid and purification on a desalting column (see Materials and Methods). A RP-HPLC chromatogram of the digest showed that I1 was devoid of the N2 (T1–T14, Cys12–Cys108) HPLC peak but retained the N1 (T8–T15, Cys62–Cys114) peak (data not shown; see Figure 2). In addition, this chromatogram contained a peak corresponding to the broad R2 peak or the Cys12-containing fragment (T1), suggesting that Cys12 was fully reduced. Reduction of this same I1 treated sample led to a chromatogram that generated new peaks consistent with R1 (T8, Cys62) and R3 (T15, Cys114) and strongly suggested that the I1 species contained an intact Cys62–Cys114 disulfide bond. Similar analysis of the intact and reduced disulfides in I2 was not successful because we could not generate enough material to characterize. It is very likely, however, that I2 contains the other disulfide pair involving an intact Cys12–Cys108 disulfide, while Cys62 and Cys114 are fully reduced. Since the relative amount of I2 is usually 10% of the I1 amount, it is likely that the Cys12–Cys108 bond is significantly more solvent exposed than the Cys62–Cys114 disulfide bond.

These reduction studies have revealed that the two disulfide bonds in IL-10 play a critical role in its structure–function properties. It appears that the Cys12–Cys108 bond is more susceptible to reduction than the Cys62–Cys114 bond. It is also likely that the partial unfolding observed for reduced

rhuIL-10 in the far-UV CD spectrum has a direct effect on the protein's loss of activity in the mast cell proliferation assay.

SUMMARY

The studies reported here were designed to quantitate and characterize the disulfide pairing in both rhuIL-10 and rmuIL-10 and to discern whether or not the disulfide bonds play a role in the proteins' expression of biological activity and/or structural stability. Chemical analysis of the free sulfhydryl content and disulfide number of CHO-derived rhuIL-10 clearly indicated the presence of two disulfide bonds and the absence of free sulfhydryl groups. Similar analysis using *E. coli*-derived rmuIL-10 indicated that it also contained two disulfide bonds and that its fifth cysteine existed as a free sulfhydryl. The disulfide bond assignments for rhuIL-10 and rmuIL-10 were elucidated through analysis of disulfide-paired peptides derived from tryptic digests using plasma desorption mass spectrometry and RP-HPLC. This analysis showed that the two disulfide pairs for both rhuIL-10 and rmuIL-10 involved the first cysteine bonded to the third and the second cysteine bonded to the fourth, that is, Cys12–Cys108 and Cys62–Cys114 for rhuIL-10 and Cys9–Cys105 and Cys59–Cys111 for rmuIL-10. We have assumed that this pairing is also identical to that of the naturally occurring IL-10s, which are not available in sufficient quantities to permit a direct comparison with the recombinant proteins.

Both rhuIL-10 and rmuIL-10 are likely to exist as a single-domain conformation, possibly globular, since complete tryptic digestion occurred only in the presence of a denaturant. On the basis of the far-UV circular dichroism studies the potentially compact rhuIL-10 and rmuIL-10 proteins were determined to have a high α-helix content (i.e., *ca.* 60%). Intact disulfides were found to be required for both proteins to retain biological activity. The loss in biological activity appears to coincide with a loss in α-helix content, as observed for the fully reduced sample in the far-UV CD. In addition, the two disulfide bonds in rhuIL-10 are readily reduced under non-denaturing conditions. The similarity in disulfide properties and structure–function of human and murine IL-10 is consistent with the high degree of amino acid sequence identity and conservation of the cysteine positions between the two proteins.

The biochemical and biophysical properties of IL-10 described above are very similar to those exhibited by several other cytokines. In particular, these properties are strikingly similar to those of human interleukin 2 (McKay, 1992), human interleukin 4 (Powers et al., 1992; Smith et al., 1992; Walter et al., 1992b), human granulocyte–macrophage colony-stimulating factor (Walter et al., 1992a; Diederichs et al., 1991), murine β interferon (Senda et al., 1992), human growth hormone (DeVos et al., 1992), and human γ interferon (Ealick et al., 1991), each of which has a known three-dimensional structure that is highly α-helical, 42–65%. Except for γ interferon, these cytokines are also highly compact single-domain structures which contain disulfide bonds that are required for both biological and structural stability. The disulfide bonds in these known structures most often lie within exposed turn or loop regions. This situation may be similar for interleukin 10 especially since the disulfide bonds were readily reduced under non-denaturing conditions. On the basis of the partial reduction studies (Figure 4) it appears that the Cys12–Cys108 disulfide bond is more solvent exposed than the Cys62–Cys114 bond. This information should provide a valuable constraint in generating structural models of IL-10.

The three-dimensional structures of these α-helical cytokines have a conserved secondary structure core containing a four α-helix motif with an up-up-down-down alignment. This conserved three-dimensional structure occurs despite the lack of any significant primary sequence homology. Interleukin 10 also has no apparent sequence homology with these cytokines, including a lack of cysteine homology; however, it does have many fundamental similarities with respect to its biochemical and biophysical properties, and thus its structure may also contain the conserved four α-helix motif. The exact location of the disulfide bonds and other aspects of the three-dimensional structure of IL-10 will depend on more detailed structural studies by X-ray crystallography or multidimensional NMR.

ACKNOWLEDGMENT

We gratefully acknowledge the contributions of Drs. Susan Cannon-Carlson, Gary Vellekamp, and Chuan-Chu Chou and the departments of Biotechnology-Development, Biotechnology-Bioanalytical, and Biotechnology-Molecular Biology within Schering-Plough Research Institute for the expression and purification of recombinant huIL-10 and muIL-10. We also thank Dr. T. L. Nagabhushan for his critical review of the manuscript.

REFERENCES

Banchereau, J., de Paoli, P., Valle, A., Garcia, E., & Rousset, F. (1991) *Science 251*, 70–72.
Chang, C. T., Wu, C.-S. C., & Yang, J. T. (1978) *Anal. Biochem. 91*, 13–31.
Chou, P. Y., & Fasman, G. D. (1978) *Adv. Enzymol. 47*, 45–148.
Damodaran, S. (1985) *Anal. Biochem. 145*, 200–204.
DeFrance, T., Vanbervliet, B., Biere, F., Durand, I., Rousset, F., & Banchereau, J. (1992) *J. Exp. Med. 175*, 671–682.
DeVos, A. M., Ultsch, M., & Kossiakoff, A. A. (1992) *Science 255*, 306–312.
de Wall Malefyt, R., Abrams, J., Bennett, B., Figdor, C., & de Vries, J. (1991) *J. Exp. Med. 174*, 1209–1220.
Diederichs, K., Boone, T., & Karplus, P. A. (1991) *Science 254*, 1779–1782.
Ealick, S. E., Cook, W. J., Vijay-Kumar, S., Carson, M., Nagabhushan, T. L., Trotta, P. P., & Bugg, C. E. (1991) *Science 252*, 698–702.
Fiorentino, D. F., Bond, M. W., & Mosmann, T. R. (1989) *J. Exp. Med. 170*, 2081–2095.
Fiorentino, D. F., Zlotnik, A., Vieira, P., Mosmann, T. R., Howard, M., Moore, K. W., & O'Garra, A. (1991) *J. Immunol. 146*, 3444–3451.
Garnier, J., Osguthorpe, D. J., & Robson, B. (1978) *J. Mol. Biol. 120*, 97–120.
Garrett, D. S., Powers, R., Marsh, C. J., Frieden, E. A., Clore, G. M., & Gronenborn, A. (1992) *Biochemistry 31*, 4347–4353.
Grassetti, D. R., & Murray, J. F. (1967) *Arch. Biochem. Biophys. 119*, 41–49.
Howard, M., O'Garra, A., Ishida, H., de Wall Malefyt, R., & de Vries, J. (1992) *J. Clin. Immunol. 12*, 239–247.
McKay, D. B. (1992) *Science 257*, 412–413.
Moore, K. W., Vieiram, P., Fiorentino, D. F., Trounstine, M. L., Khan, T. A., & Mosmann, T. R. (1990) *Science 248*, 1230–1234.
Moore, K. W., O'Garra, A., de Wall Malefyt, R., Vieira, P., & Mosmann, T. (1993) *Annu. Rev. Immunol.* (in press).
O'Garra, A., Stapelton, G., Dhar, V., Pearce, M., Schumacher, J., Rugo, H., Barbis, D., Stall, A., Cupp, J., Moore, K., Vieira, P., Mosmann, T., Whitmore, A., Arnold, L., Haughton, G., & Howard, M. (1990) *Int. Immunol. 2*, 821–832.

Powers, R., Garrett, D. S., March, C. J., Frieden, E. A., Gronenborn, A. M., & Clore, G. M. (1992) *Science 256*, 1673–1677.

Rousset, F., Garcia, E., DeFrance, T., Peronne, C., Hsu, D.-H., Kastelein, R., Moore, K. W., & Banchereau, J. (1992) *Proc. Natl. Acad. Sci. U.S.A. 89*, 1890–1893.

Senda, T., Shimazu, T., Matsuda, S., Kawano, G., Shimizu, H., Nakamura, K. T., & Mitsui, Y. (1992) *EMBO J. 11*, 3193–3201.

Smith, L. J., Redfield, C., Boyd, J., Lawrence, G. M. P., Edwards, R. G., Smith, R. A. G., & Dobson, C. M. (1992) *J. Mol. Biol. 224*, 899–904.

Sundqvist, B., Kamensky, I., Hakansson, P., Kjellberg, J., Salehpour, M., Widdiyasekera, S., Fohlman, J., Peterson, P. A., & Roepstorff, P. (1984) *Biomed. Mass Spectrom. 11*, 242–257.

Takakuwa, T., Konno, T., & Meguro, H. (1985) *Anal. Sci. 1*, 215–218.

Thannhauser, T. W., Konishi, Y., & Scheraga, H. A. (1984) *Anal. Biochem. 138*, 181–188.

Tsarbopoulos, A. (1989) *Pept. Res. 2*, 258–266.

Tsarbopoulos, A., Becker, G. W., Occolowitz, J. L., & Jardine, I. (1988) *Anal. Biochem. 171*, 113–123.

Vieira, P., de Wall Malefyt, R., Dang, M.-N., Johnson, K. E., Kastelein, R., Fiorentino, D. F., deVries, J. E., Roncarolo, M.-G., Mosmann, T. R., & Moore, K. W. (1991) *Proc. Natl. Acad. Sci. U.S.A. 88*, 1172–1176.

Walter, M. R., Cook, W. J., Ealick, S. E., Nagabhushan, T. L., Trotta, P. P., & Bugg, C. E. (1992a) *J. Mol. Biol. 224*, 1075–1085.

Walter, M. R., Cook, W. J., Zhao, B. G., Cameron, R., Ealick, S. E., Walter, R., Reichert, P., Nagabhushan, T. L., Trotta, P. P., & Bugg, C. E. (1992b) *J. Biol. Chem. 267*, 20371–20376.

Windsor, W. T., Syto, R., Le, H., & Trotta, P. P. (1991) *Biochemistry 30*, 1259–1264.